Eur Radiol
DOI 10.1007/s00330-014-3512-3

HEPATOBILIARY-PANCREAS

# Differentiation of focal-type autoimmune pancreatitis from pancreatic carcinoma: assessment by multiphase contrast-enhanced CT

**Naohiro Furuhashi · Kojiro Suzuki · Yusuke Sakurai · Mitsuru Ikeda · Yuichi Kawai · Shinji Naganawa**

Received: 10 June 2014 / Revised: 30 September 2014 / Accepted: 17 November 2014


**Abstract**
*Objectives* To evaluate the utility of multiphase contrast-enhanced computed tomography (CT) findings alone and in combination for differentiating focal-type autoimmune pancreatitis (f-AIP) from pancreatic carcinoma (PC).
*Methods* The study group comprised 22 f-AIP lesions and 61 PC lesions. Two radiologists independently evaluated CT findings. Frequencies of findings were compared between f-AIP and PC. Statistical, univariate and multivariate analyses were performed.
*Results* Homogeneous enhancement during the portal phase (AIP, 59 % vs. PC, 3 %; $P<0.001$), dotted enhancement during the pancreatic phase (50 % vs. 7 %; $P<0.001$), duct-penetrating sign (46 % vs. 2 %; $P<0.001$), enhanced duct sign (36 % vs. 2 %; $P<0.001$) and capsule-like rim (46 % vs. 3 %; $P<0.001$) were more frequently observed in AIP. Ring-like enhancement during the delayed phase (5 % vs. 46 %; $P<0.001$) and peripancreatic strands with a length of at least 10 mm (5 % vs. 39 %; $P=0.001$) were more frequently observed in PC. AIP was identified with 82 % sensitivity and 98 % specificity using four of these seven findings. Multivariate analysis revealed significant differences in dotted enhancement ($P=0.004$), duct-penetrating sign ($P<0.001$) and capsule-like rim ($P=0.007$).
*Conclusions* The combination of CT findings may allow improvements in differentiating f-AIP from PC.
*Key Points*
- *f-AIP can mimic PC on imaging findings.*
- *The differentiation of f-AIP from PC is important in patient management.*
- *Some CT findings can be used to identify AIP.*
- *The combination of CT findings will improve differentiation from PC.*

**Keywords** Autoimmune pancreatitis · Pancreatic carcinoma · Differential diagnosis · Multiphase contrast-enhanced computed tomography · Multivariate analysis

**Abbreviations and acronyms**

| | |
|---|---|
| AIP | Autoimmune pancreatitis |
| CBD | Common bile duct |
| CT | Computed tomography |
| f-AIP | Focal-type autoimmune pancreatitis |
| MPD | Main pancreatic duct |
| MRI | Magnetic resonance imaging |
| PC | Pancreatic carcinoma |

## Introduction

Autoimmune pancreatitis (AIP) is now recognized as the pancreatic manifestation of immunoglobulin G4 (IgG4)-

N. Furuhashi (✉) · K. Suzuki · Y. Sakurai · S. Naganawa
Department of Radiology, Nagoya University Graduate School of Medicine, 65 Tsurumai-cho, Showa-ku, Nagoya 466-8550, Japan
e-mail: naofuru@med.nagoya-u.ac.jp

K. Suzuki
e-mail: kojiro@med.nagoya-u.ac.jp

Y. Sakurai
e-mail: y-sakurai@med.nagoya-u.ac.jp

S. Naganawa
e-mail: naganawa@med.nagoya-u.ac.jp

M. Ikeda
Department of Radiological Technology, Nagoya University Graduate School of Medicine, 1-20 Daikominami 1-chome, Higashi-ku, Nagoya 461-8673, Japan
e-mail: mikeda@nagoya-u.jp

Y. Kawai
Department of Diagnostic Radiology, Japanese Red Cross Nagoya Daiichi Hospital, 3-35 Michishita-cho, Nakamura-ku, Nagoya 453-8551, Japan
e-mail: y-kawai@nagoya-1st.jrc.or.jp

Published online: 30 November 2014

related sclerosing disease [1]. A diffuse sausage-shaped enlargement of the pancreas and capsule-like rim on computed tomography (CT) are considered to be characteristic of AIP [2, 3]. Therefore, AIP can be suspected when these characteristic findings are present.

However, AIP is often accompanied by focal pancreatic enlargement or abnormal enhancement [2, 4], and this focal-type AIP (f-AIP) can mimic pancreatic carcinoma (PC) on imaging findings [5, 6]. AIP may also symptomatically resemble PC because AIP patients may have abdominal pain, obstructive jaundice and weight loss. Furthermore, completely different treatment strategies are used for AIP and PC. AIP responds effectively to steroid therapy [7], whereas PC is typically treated by surgical resection and/or chemotherapy. Therefore, differentiating these two entities is important to avoid unnecessary pancreatic resections.

AIP is diagnosed using CT, magnetic resonance imaging (MRI), serological and histological findings, and additionally, the response to steroid therapy [8, 9]. Elevations in serum IgG4 levels are characteristic of AIP; however, serum IgG4 levels are mildly elevated in approximately 10 % of PC patients [10] and are often normal in AIP patients [11]. Although pancreatic biopsy is useful for differentiating between AIP and PC, it is an invasive procedure that may not be able to completely exclude PC when pancreatitis is suspected [12, 13].

CT is the most commonly used imaging technique when pancreatic disease is suspected, and is the first step to diagnosing AIP. Therefore, identifying the CT findings that can be used to differentiate f-AIP from PC is of importance. Although previous studies already identified some findings [14–17], they only demonstrated the utility of each finding alone, the sensitivity of which was not high, while some findings offered high specificity as a whole. Higher sensitivity is needed in order to avoid unnecessary pancreatic resections. To the best of our knowledge, one previous study examined the combination of findings for differentiating f-AIP from PC. However, a combination of CT and MRI findings was used, and the number of patients in the AIP group was relatively low ($n$=11). Therefore, we evaluated the accuracy of each CT finding alone and in combination for a differential diagnosis between f-AIP and PC.

## Materials and methods

### Patients

Our institutional review board approved the retrospective collection of data and analysis for this study, and the need for informed consent from patients was waived. CT examinations were performed in accordance with the established clinical standards of our institution, and each patient agreed to undergo an examination after the purpose, methods and risks were fully explained.

Our institution holds a prospectively maintained database of patients referred for CT examinations for a detailed evaluation of the pancreas and biliary system. Through the database, we retrospectively identified consecutive 22 f-AIP patients who were diagnosed on the basis of the International Consensus Diagnostic Criteria (ICDC) for AIP [8] or Revised Japanese Pancreas Society criteria of AIP [9] between January 2007 and August 2012. A ‘focal’ lesion was defined as ‘a mass-forming, focal enlargement or abnormal enhancement of the pancreas within a third of the pancreas’. Sixty-four consecutive patients with invasive PC lesions who were histopathologically diagnosed using surgically resected specimens were also selected between November 2010 and August 2012.

Patients who had a history of pancreatic surgery (f-AIP; $n$=1), whose CT images were poor because of a failure to hold a breath or body motion (PC; $n$=2), who underwent stenting in the main pancreatic duct (PC; $n$=1) and who had both diffuse-type AIP and PC (PC; $n$=1) were excluded from this study group. Therefore, the present study groups comprised 21 patients with f-AIP (20 men, 1 woman; mean age, 66.7 years; range, 55–79 years) and 60 patients with PC (36 men, 24 women; mean age, 65.8 years; range, 38–82 years) (Table 1). In the f-AIP group, 19 patients were diagnosed on the basis of ICDC, 18 of whom had type 1 AIP (definite, 13; probable, 5) and one had type 2 (probable). Twenty patients were diagnosed on the basis of the Japanese diagnostic criteria (definite, 14; probable, 6). Eighteen patients were diagnosed with both ICDC and the Japanese criteria, one was diagnosed with ICDC alone and two were diagnosed with the Japanese criteria alone. All patients with f-AIP underwent CT examinations before receiving therapy. One patient with f-AIP and one patient with PC had two masses each; one lesion was located within the pancreatic head and the other was within the pancreatic tail in both cases. Therefore, we evaluated 22 f-AIP and 61 PC lesions.

Three f-AIP patients underwent surgical pancreatic resection because PC was suspected prior to surgery. The other f-AIP patients received steroid therapy in our institute and showed the complete resolution or marked improvements on imaging or in the clinical follow-up. Fifty-eight PC lesions were histopathologically identified as tubular adenocarcinomas, and three were adenosquamous carcinomas.

### Laboratory data

Serum levels of IgG4 and carbohydrate antigen 19-9 (CA19-9) were collected from medical records if available.

**Table 1** Patient characteristics, laboratory data, and the size and location of the lesions in patients with focal-type autoimmune pancreatitis (f-AIP) and pancreatic carcinoma (PC)

| | f-AIP | PC | *P* |
|---|---|---|---|
| Select period | Jan. 2007–Aug. 2012 | Nov. 2010–Aug. 2012 | |
| No. of patients | 21 | 60 | |
| No. of lesions | 22 | 61 | |
| Mean age (range) | 66.7 (55–79) | 65.8 (38–82) | 0.739 |
| Male-to-female ratio | 20:1 | 36:24 | 0.002 |
| Laboratory data | | | |
| IgG4 (mg/dL)[a] | 245±360 [88–1,310][b] | 82±62 [29–162][b] | 0.008 |
| CA19-9 (U/mL) | 51±125 [1–586][b] | 1,359±3,914 [1–28,160][b] | 0.012 |
| Size of the lesions (mm) | 35±11 [18–55][b] | 25±9 [10–47][b] | <0.001 |
| Location of the lesions | | | 0.263 |
| Head | 18 (82 %) | 45 (74 %) | |
| Body | 1 (5 %) | 11 (18 %) | |
| Tail | 3 (13 %) | 5 (8 %) | |

[a] Data were available in 12 AIP and 4 PC patients

[b] Data are the mean±standard deviation [range]

### CT image acquisition

CT examinations were performed using a 64-channel multisection CT system (Aquilion, Toshiba Medical Systems, Tokyo, Japan). Non-ionic contrast material (2.0–2.5 mL/kg) with an iodine concentration of 300 mg/mL was injected through the peripheral venous line within 30 s (with an upper limit of 5 mL/s), and a saline flush was injected at a fixed rate of 5 mL/s within 5 s immediately after the injection of contrast material. After unenhanced images had been acquired, all patients underwent pancreatic, portal and delayed phase imaging. Individualized scan delays were determined using the automatic bolus-tracking method (SureStart, Toshiba Medical Systems). Average scan delays from the injection of contrast material to the start of pancreatic, portal and delayed phase imaging were 44, 75 and 210 s, respectively. CT image analysis was performed using unenhanced images with a 5-mm section thickness at 5-mm intervals and both axial and coronal reformatted enhanced images with a 2-mm section thickness at 2-mm intervals.

### CT image analysis

Two radiologists (6 and 16 years of experience in the interpretation of abdominal imaging), who were blinded to the final diagnosis and other examination findings and were aware that the cohort included f-AIP and PC patients, independently evaluated multiphase contrast-enhanced CT findings in each patient. In cases where the readers disagreed, a final consensus decision was reached through discussion. The maximum diameter of the lesions decided by the two radiologists was measured at a workstation using electronic calipers in axial and coronal images.

Regarding assessments of the affected pancreatic area, (a) the location of the lesion (head, body or tail of the pancreas) and (b) enhancement patterns during the pancreatic, portal and delayed phases were analysed. Homogeneity (homogeneous or heterogeneous) and the degree of enhancement (hypoattenuation was defined as decreased enhancement, and iso- or hyperattenuation was defined as good enhancement, compared to the unaffected surrounding parenchyma of the pancreas) in the enhancement patterns were evaluated and divided into the following four categories: homogeneous enhancement, homogeneous decreased enhancement, heterogeneous enhancement or heterogeneous decreased enhancement. Regarding the enhancement of lesions, (c) a dotted enhancement during the pancreatic phase (Fig. 1) and (d) ring-like enhancement during the delayed phase (Fig. 2) were also evaluated. A dotted enhancement was defined as the presence of dotted or speckled hyperattenuation areas relative to that of the surrounding lesions. Furthermore, the following findings were analysed in all images: (e) duct-penetrating sign (Fig. 3): detection of the main pancreatic duct (MPD) lumen in the lesions and, if the MPD lumen was detected in the lesions, the length of the visible lumen in the affected area was noted as more than half or less than half; (f) enhanced duct sign (Fig. 4): wall enhancement of MPD in the lesion and, if detected, their phases were noted; (g) capsule-like rim: a low-attenuation rim surrounding adipose tissue; (h) calcification; (i) cyst formation; (j) vascular involvement, which was defined as stenosis or obstruction of vessels, or the presence of soft tissue or a tumour abutting at least half the circumference of the vessels (celiac, superior mesenteric or splenic artery,

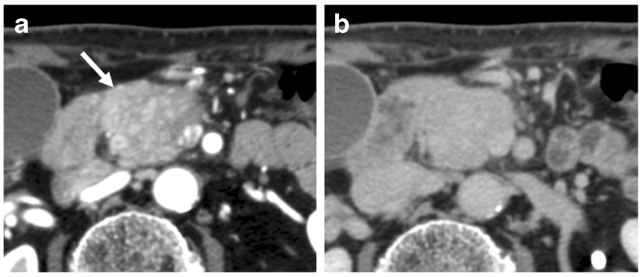


**Fig. 1** A man in his seventies with f-AIP in the pancreatic head. **a** Axial CT image during the pancreatic phase shows a focal enlargement in the pancreatic head and a dotted enhancement in the decreased enhanced area (*arrow*). **b** The lesion shows a homogeneous enhancement during the delayed phase

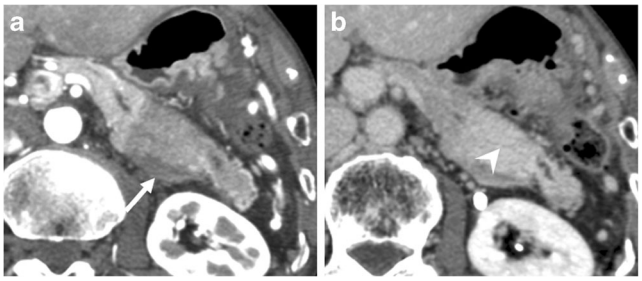


**Fig. 3** A man in his seventies with f-AIP in the pancreatic tail. **a** Axial CT image during the pancreatic phase shows a heterogeneously decreased enhancement. A capsule-like rim is shown as a hypoattenuating rim in the surrounding adipose tissue (*arrow*). **b** The lesion shows a homogeneous enhancement during the delayed phase. The lumen of the main pancreatic duct (*arrowhead*) can be detected within the lesion. This was defined as a 'duct-penetrating sign'

and main portal, superior mesenteric or splenic vein); and (k) peripancreatic strands with a length of at least 10 mm (Fig. 2): "peripancreatic strands" were defined as the linear soft tissue structure originating from the lesion and extending into the surrounding adipose tissue.

Regarding the unaffected pancreatic assessment, (a) dilation of upstream MPD (more than 3 mm) and (b) distal atrophy of the pancreatic parenchyma were evaluated. Lesions located at the edge of the pancreatic tail were excluded when evaluations were performed.

With regard to the biliary system, (a) a tube or stent in the common bile duct (CBD) or CBD stenosis, which was considered to be positive when the lumen of CBD was narrow and the bile duct above the stenosis was dilated at least 10 mm, were evaluated for lesions located in the pancreatic head. Moreover, regarding lesions without a CBD stent or tube, (b) CBD stenosis, (c) incomplete visualization of the CBD lumen, (d) thickened CBD wall and (e) enhanced CBD wall were evaluated.

## Statistical analysis

Intergroup comparisons between f-AIP and PC were performed using Fisher's exact test for categorical variables and the Student's *t* test for numeric variables. The sensitivity, specificity, accuracy and odds ratio of differentiating between f-AIP and PC were calculated for CT findings that were significantly different and the combination of these findings. The CT finding that showed the most significant difference among enhancement patterns in all phases, and other findings

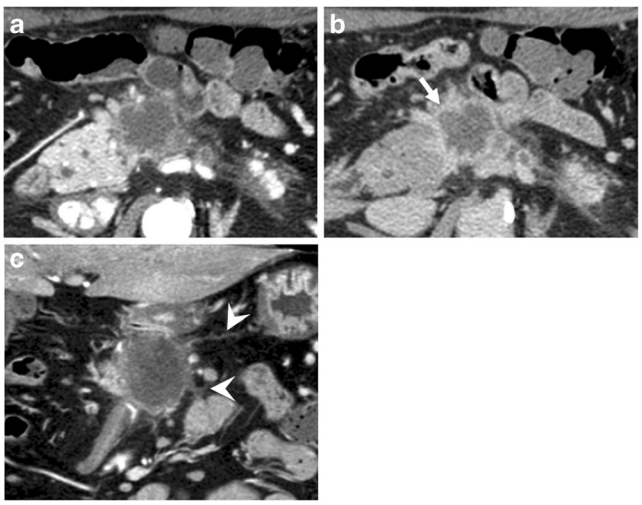


**Fig. 2** A man in his seventies with PC in the pancreatic body. **a** and **b** show axial CT images during the pancreatic and delayed phases, and the tumor shows a heterogeneously decreased enhancement in the central part and ring-like enhancement in the peripheral part (*arrow*) during the delayed phase. **c** The peripancreatic strands deriving from the lesion and extending into the surrounding adipose tissue are shown in the coronal reconstructed CT image and the lengths of the strands are over 10 mm (*arrowheads*)

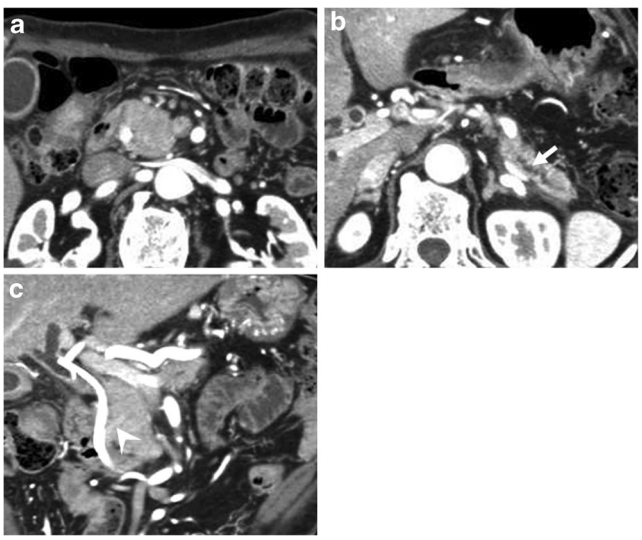


**Fig. 4** A man in his eighties with f-AIP in the pancreatic head. **a** and **b** show axial CT images and **c** shows a coronal reconstructed image during the pancreatic phase. **a** A focal pancreatic enlargement and heterogeneous decreased enhancement are seen in the pancreatic head. **b** MPD dilation (*arrow*) and distal atrophy are observed in the pancreatic tail. **c** An enhancement of the MPD wall is seen in the lesion (*arrowhead*) and this was defined as an 'enhanced duct sign'

that showed significant differences between groups were chosen to evaluate the combination. Furthermore, univariate and multivariate logistic regression analyses were performed in order to determine which combination of findings was useful for differentiating between f-AIP and PC. Findings that were not significantly different and correlated with each other by univariate analyses were excluded from multivariate analysis.

The kappa (κ) statistic was used to measure interobserver agreement in the evaluation of CT findings. A κ value of less than 0.20 was considered to indicate poor agreement; 0.21–0.40, fair agreement; 0.41–0.60, moderate agreement; 0.61–0.80, good agreement; and 0.81–1.00, very good agreement.

We used SPSS 20 software (SPSS, Chicago, IL) for statistical analyses and adopted 5 % as a significance level for all statistical tests. Mean data are expressed as means±standard deviations with their range in brackets.

## Results

### Laboratory data

Serum IgG4 levels were obtained in 12 f-AIP and 4 PC patients and were significantly higher in f-AIP patients (245±360 [88–1,310] mg/dL, mean±standard deviation [range]) than in PC patients (82±62 [29–162] mg/dL) in PC ($P$=0.008). CA19-9 was measured in all 21 f-AIP and 60 PC patients and was significantly higher in PC patients (1,359±3,914 [1–28,160] U/mL) than in f-AIP patients (51±125 [1–586] U/mL) ($P$=0.012) (Table 1).

### CT findings

The frequencies of CT findings are listed in Tables 1 and 2. Eighteen lesions (82 %) in f-AIP patients were located in the pancreatic head, one (5 %) in the pancreatic body and three (13 %) in the pancreatic tail. In PC patients, 45 lesions (74 %) were located in the pancreatic head, 11 (18 %) in the pancreatic body and five (8 %) in the pancreatic tail. The mean size of the lesions was significantly larger in f-AIP patients (35±11 [18–55] mm) than in PC patients (25±9 [10–47] mm) ($P$<0.001).

As shown in Table 2, f-AIP was more likely to show a homogeneous enhancement during the portal and delayed phases (59 % vs. 3 % [f-AIP vs. PC], $P$<0.001, during the portal phase; 86 % vs. 41 %, $P$<0.001, during the delayed phase). In contrast, PC was more like to show a heterogeneously decreased enhancement (23 % vs. 84 % [f-AIP vs. PC], $P$<0.001, in the portal phase; 0 % vs. 36 %, $P$<0.001, in the delayed phase). The frequency by which a dotted enhancement during the pancreatic phase, duct-penetrating sign, enhanced duct sign and capsule-like rim was observed was significantly higher in f-AIP than in PC (50 % vs. 7 % [f-AIP vs. PC], $P$<0.001; 46 % vs. 2 %, $P$<0.001; 36 % vs. 2 %, $P$<0.001; 46 % vs. 3 %, $P$<0.001, respectively). Ten f-AIP lesions showed the duct-penetrating sign; five lesions had a detectable MPD lumen with a length of more than half of the lesion, and five lesions had a detectable MPD lumen with a length of less than half of the lesion. In PC, one lesion showed the duct-penetrating sign with a length of more than half of the lesion. The enhanced duct sign was detected in eight f-AIP lesions during the portal phase and in six lesions (75 %) during the pancreatic phase, while no lesion presented this sign during the delayed phase. In contrast, one PC lesion showed the enhanced duct sign during the pancreatic phase. The frequency by which a ring-like enhancement during the delayed phase and peripancreatic strands were observed was significantly higher in PC than in f-AIP (5 % vs. 46 % [f-AIP vs. PC], $P$<0.001; 5 % vs. 39 %, $P$=0.001, respectively). No significant difference was observed in the frequencies of calcification, cyst formation, vascular involvement, upstream dilation of MPD or distal atrophy between f-AIP and PC.

Regarding lesions located in the pancreatic head, stenting/tubing in CBD or CBD stenosis was observed in 72 % (13/18) of f-AIP and 64 % (29/45) of PC, with no significant differences being noted between groups ($P$=0.389). CBD stents/tubes were detected in 7 f-AIP and 17 PC lesions. In pancreatic head lesions without a CBD stent or tube (11 f-AIP and 28 PC lesions), no significant difference was observed in CBD stenosis (55 % vs. 43 % [f-AIP vs. PC], $P$=0.380), incomplete visualization of the CBD lumen (9 % vs. 25 %, $P$=0.262), thickened CBD wall (45 % vs. 28 %, $P$=0.262) or enhanced CBD wall (45 % vs. 36 %, $P$=0.418) between f-AIP and PC.

Table 3 shows the significant findings used to differentiate f-AIP from PC and their sensitivity, specificity, accuracy and odds ratio. A ring-like enhancement and peripancreatic strands were treated as negative findings. None of these individual findings were able to achieve high sensitivity and high specificity. However, 82 % sensitivity, 98 % specificity, 94 % accuracy and the highest odds ratio (270.0; 95 % confidence intervals, 28.4–2,571.2) were obtained when any four of the seven findings were combined. Furthermore, these significant findings showed moderate-to-good interobserver agreement (κ=0.41–0.70).

The following eight findings were selected as candidates for the multivariate logistic regression analysis: a homogeneous enhancement during the portal phase, homogeneous enhancement during the delayed phase, dotted enhancement during the pancreatic phase, ring-like enhancement during the delayed phase, duct-penetrating sign, enhanced duct sign, capsule-like rim and peripancreatic strands. The following four findings were then selected using a stepwise method for the final prediction model: a dotted enhancement during the pancreatic phase, duct-penetrating sign, capsule-like rim and peripancreatic strands. Finally, a dotted enhancement ($P$=

**Table 2** Frequencies of CT findings in 22 f-AIP and 61 PC lesions

| Findings | f-AIP | PC | Kappa | *P* |
|---|---|---|---|---|
| Pancreatic affected area | | | | |
| Enhancement during the pancreatic phase | | | 0.24 | |
| Homogeneous | 1 (5 %) | 1 (2 %) | | 0.462 |
| Homogeneous decreased | 5 (23 %) | 2 (3 %) | | 0.012 |
| Heterogeneous | 1 (5 %) | 1 (2 %) | | 0.462 |
| Heterogeneous decreased | 15 (67 %) | 57 (94 %) | | 0.006 |
| Enhancement during the portal phase | | | 0.50 | |
| Homogeneous | 13 (59 %) | 2 (3 %) | | <0.001 |
| Homogeneous decreased | 3 (13 %) | 6 (10 %) | | 0.444 |
| Heterogeneous | 1 (5 %) | 2 (3 %) | | 0.608 |
| Heterogeneous decreased | 5 (23 %) | 51 (84 %) | | <0.001 |
| Enhancement during the delayed phase | | | 0.70 | |
| Homogeneous | 19 (86 %) | 25 (41 %) | | <0.001 |
| Homogeneous decreased | 2 (9 %) | 2 (3 %) | | 0.285 |
| Heterogeneous | 1 (5 %) | 12 (20 %) | | 0.085 |
| Heterogeneous decreased | 0 | 22 (36 %) | | <0.001 |
| Dotted enhancement during the pancreatic phase | 11(50 %) | 4 (7 %) | 0.41 | <0.001 |
| Ring-like enhancement during the delayed phase | 1 (5 %) | 28 (46 %) | 0.54 | <0.001 |
| Duct-penetrating sign | 10 (46 %) | 1 (2 %) | 0.55 | <0.001 |
| Enhanced duct sign | 8 (36 %) | 1 (2 %) | 0.55 | <0.001 |
| Capsule-like rim | 10 (46 %) | 2 (3 %) | 0.49 | <0.001 |
| Calcification | 0 | 3 (5 %) | 1 | 0.392 |
| Cyst formation | 5 (23 %) | 21 (34 %) | 0.75 | 0.934 |
| Vascular involvement | 6 (27 %) | 25 (41 %) | 0.82 | 0.254 |
| Peripancreatic strands (≥10 mm) | 1 (5 %) | 24 (39 %) | 0.64 | 0.001 |
| Pancreatic unaffected area | | | | |
| MPD upstream dilation (>3 mm)[a] | 14/20 (70 %) | 48/58 (83 %) | 0.81 | 0.934 |
| Distal atrophy[a] | 7/20 (35 %) | 22/58 (38 %) | 0.73 | 0.518 |
| Bile duct | | | | |
| Stent/tube+or stenosis[b] | 13/18 (72 %) | 29/45 (64 %) | 0.66 | 0.389 |
| Stenosis[c] | 6/11 (55 %) | 12/28 (43 %) | 0.51 | 0.380 |
| Incomplete visualization of the CBD lumen[c] | 1/11 (9 %) | 7/28 (25 %) | 0.41 | 0.262 |
| Thickened CBD wall[c] | 5/11 (45 %) | 8/28 (28 %) | 0.40 | 0.262 |
| Enhanced CBD wall[c] | 5/11 (45 %) | 10/28 (36 %) | 0.57 | 0.418 |

*MPD* main pancreatic duct, *CBD* common bile duct

[a] Lesions located in the edge of the pancreatic tail were excluded

[b] Lesions in the pancreatic head were evaluated and CBD stents/tubes were detected in 7 f-AIP and 17 PC lesions

[c] Lesions in the pancreatic head were evaluated and these patients did not have CBD stents/tubes

0.004), duct-penetrating sign ($P<0.001$) and capsule-like rim ($P=0.007$) were identified as significant predictors.

## Discussion

f-AIP can mimic PC on imaging findings. CT is the most commonly used imaging technique when a pancreatic mass is suspected; therefore, it is extremely important to understand which CT findings are useful for differentiating these two entities because patient management is completely different for each disorder. Several CT findings were previously reported to be characteristic of AIP or were more frequently observed in AIP than in PC [2–4, 14, 16–20]. Some CT findings showed high specificity for differentiating AIP from PC, but relatively low sensitivity as a whole [14, 16, 17,

**Table 3** The sensitivity, specificity, accuracy and odds ratio of significant findings and their combination for differentiating f-AIP from PC

| | Findings | Sensitivity[a] | Specificity[a] | Accuracy[a] | Odds ratio[b] |
|---|---|---|---|---|---|
| i | Homogeneous enhancement during the portal phase | 0.59 (13/22) | 0.97 (59/61) | 0.88 (72/82) | 42.6 (8.2–220.9) |
| ii | Dotted enhancement during the pancreatic phase | 0.50 (11/22) | 0.93 (57/61) | 0.82 (68/83) | 14.2 (3.8–53.0) |
| iii | Duct-penetrating sign | 0.46 (10/22) | 0.98 (60/61) | 0.84 (70/83) | 50.0 (5.8–428.0) |
| iv | Enhanced duct sign | 0.36 (8/22) | 0.98 (60/61) | 0.82 (68/83) | 34.3 (4.0–296.9) |
| v | Capsule-like rim | 0.46 (10/22) | 0.97 (59/61) | 0.83 (69/83) | 24.6 (4.8–126.8) |
| vi | Absence of a ring-like enhancement | 0.95 (21/22) | 0.46 (28/61) | 0.59 (49/83) | 17.8 (2.3–141.0) |
| vii | Absence of peripancreatic strands | 0.95 (21/22) | 0.39 (24/61) | 0.54 (45/83) | 13.6 (1.7–108.0) |
| | Combination of 3/7 findings | 0.91 (20/22) | 0.93 (57/61) | 0.93 (77/83) | 142.5 (24.2–838.4) |
| | Combination of 4/7 findings | 0.82 (18/22) | 0.98 (60/61) | 0.94 (78/83) | 270.0 (28.4–2,571.2) |

[a] Data are in terms of percentages and the numbers in parentheses refer to the number of lesions

[b] The ranges in parentheses refer to 95 % confidence intervals

21]. We speculated that the combination of individual findings could increase sensitivity.

In the present study, a homogeneous enhancement during the portal phase, dotted enhancement during the pancreatic phase, duct-penetrating sign, enhanced duct sign and capsule-like rim showed high specificities (greater than 90 %), but relatively low sensitivities (less than 60 %) in differentiating f-AIP from PC. In addition to these findings, a ring-like enhancement during the delayed phase and peripancreatic strands, the frequencies of which were significantly higher in PC, were used as negative findings when evaluating the combination of CT findings. By combining four of the seven significant CT findings, 82 % sensitivity, 98 % specificity and 94 % accuracy were achieved for differentiating f-AIP from PC.

f-AIP was more likely to show a homogeneous enhancement during the portal and delayed phases. Previous studies also showed that AIP was more likely to show a homogeneous enhancement during these phases [16, 17, 21], which is consistent with the results of the present study. The sensitivity of the homogeneous enhancement was higher in the delayed phase than in the portal phase; in contrast, its specificity was higher in the portal phase than in the delayed phase.

Sugiyama et al. [22] reported that the frequency by which a dotted enhancement was observed during the pancreatic phase on contrast-enhanced fat-suppressed T1-weighted images on MRI was significantly higher in f-AIP than in PC (85 % vs. 5 %). In this study, the frequency by which a dotted enhancement was observed during the pancreatic phase was significantly higher in f-AIP (50 % vs. 7 %), and this finding will be useful for differentiating f-AIP from PC. The enhanced area in the pancreatic phase may reflect residual normal or mildly involved pancreatic lobules within AIP lesions [23]. These frequencies were different (50 % vs. 85 %) from those reported in a study using MRI by Sugiyama et al. Differences in these modalities, such as MRI offering higher contrast images than CT, may have contributed to these inconsistencies.

The frequency by which a ring-like enhancement was observed during the delayed phase was significantly higher in PC than in f-AIP. As reported previously [22, 24, 25], an internally decreased enhanced area reflects the presence of an abundant fibrous stroma within a tumour, making the tumour hypovascular with cystic or necrotic components, whereas a peripherally enhanced area reflects inflammatory cell invasion or fibrous tissue as well as tumour cells.

Ichikawa et al. [26] demonstrated that a duct-penetrating sign during magnetic resonance cholangiopancreatography (MRCP) was useful for differentiating inflammatory pancreatic masses from PC. In this study, the frequency by which the duct-penetrating sign was observed was significantly higher in f-AIP than in PC. This sign may indicate that MPD is narrowed, but not obstructed in f-AIP, whereas PC easily makes MPD obstructed; therefore, it may be a useful finding for differentiating f-AIP from PC. Since the length of the detectable MPD lumen was sometimes shortened, it is important to observe MPD carefully in lesions.

Previous studies reported that the MPD wall enhancement, termed an ‘enhanced duct sign’, was useful for identifying AIP [19, 20]. However, in a previous study to evaluate the frequency of the enhanced duct sign, the AIP group comprised both diffuse and focal-type AIP. In the present study, its frequency was compared between ‘focal-type’ AIP and PC, and high specificity (98 %) was achieved. Therefore, we considered this sign to be useful not only for diagnosing AIP but also for differentiating f-AIP from PC. Our results indicated that this finding may histopathologically reflect periductal inflammatory changes and correlate with the degree of inflammation because the characteristic histopathological findings of AIP are known to include periductal lymphoplasmacytic infiltrates and storiform fibrosis [27, 28].

However, the correlation between CT and histopathological findings was not evaluated in the present study.

A capsule-like rim was detected in 46 % of f-AIP lesions. In previous studies, 40–64 % of f-AIP lesions had a capsule-like rim [14, 17, 21], which was consistent with the results of the present study.

Peripancreatic strands were reported as the finding that reflected inflammatory reactions in AIP [2], whereas this finding was also reported to correspond with extrapancreatic carcinoma invasion with marked fibrotic thickening of adipose tissue septa for PC [29]. Takahashi et al. [14] reported that the frequency by which peripancreatic strands was observed was significantly higher in AIP than in PC (70 % vs. 27 %), whereas Chang et al. [16] found no significant differences in its frequency (43 % vs. 65 %). Neither study described the length of the strands. The cut-off value of these strands was defined as 10 mm in this study because Yang et al. reported that peripancreatic strands that were more than 10 mm in length were absent in their AIP group [4]. Based on this finding, the frequency by which peripancreatic strands were observed was significantly higher in the PC group than in the f-AIP group (5 % vs. 39 %).

Several previous studies demonstrated that upstream MPD dilation was more frequent in PC than in AIP [14, 16, 17, 21], and their cut-off values depended on the authors' choice (4 or 5 mm). The cut-off value of the MPD diameter in the present study was 3 mm because its normal diameter was previously reported to be 1–3 mm [30], and no significant difference was observed between f-AIP and PC. Distal atrophy did not significantly differ between f-AIP and PC, while other studies showed that its frequency was significantly higher in PC than in f-AIP [16, 17, 21].

Calcification has often been reported in AIP, especially in cases that relapse [31], and its frequency was shown to be significantly higher in AIP than in PC [14]. However, calcification was not detected in any of the patients in the f-AIP group and no significant difference was observed between f-AIP and PC. No significant difference was also noted in the formation of cysts or vascular involvement between f-AIP and PC, which is consistent with previous findings [14, 16, 21].

No significant differences were observed in stenting/tubing in CBD and CBD stenosis between f-AIP and PC. Moreover, no significant differences were noted in incomplete visualization of the CBD lumen and thickened or enhanced CBD wall between lesions in the pancreatic head without a CBD stent or tube. Dilation of the CBD was not significantly different between AIP and PC in previous studies [14, 16]. However, Sun et al. reported that the frequency of CBD stenosis was significantly higher in f-AIP than in PC (30 % vs. 0 %), while the frequency of the complete obstruction of CBD was significantly higher in PC than in f-AIP (0 % vs. 53 %) [17]. Takahashi et al. reported that the frequency by which the wall enhancement was observed was significantly higher in AIP than in PC (52 % vs. 6 %) [14]. Therefore, the usefulness of the CBD finding remains controversial, including in the present study.

Overall, each CT finding showed moderate-to-good interobserver agreement, whereas that of the enhancement pattern during the pancreatic phase was not high ($\kappa$=0.24). Although it is difficult to clarify the reason for this, the contrast enhancement of lesions was weaker during the pancreatic phase than the other phases and may have had an influence on subjective evaluations.

Multivariate logistic regression analysis revealed that, among the individual findings that were significantly different, a dotted enhancement, duct-penetrating sign and capsule-like rim were more useful findings for the differentiation between f-AIP and PC.

This study had several limitations. First of all, the prevalence of sex differences was not matched between the f-AIP and PC groups; the percentage of male patients in the f-AIP group was markedly higher than that in the PC group. Second, many f-AIP patients were type 1 AIP, and it remains uncertain whether the same results could be achieved for type 2 AIP. Third, the evaluation of extrapancreatic lesions, such as renal involvement and retroperitoneal fibrosis, was not included in this study. Therefore, the ability of differentiation may be improved by including extrapancreatic lesions. Furthermore, a validation study was not performed in the other institutions and more prospective studies are needed to confirm the results of this study.

In conclusion, the combination of CT findings that are frequently detected in AIP and PC can achieve high sensitivity and high specificity in differentiating f-AIP from PC. A differential diagnosis should be made using not only individual CT findings but also a combination.

**Acknowledgements** The scientific guarantor of this publication is Shinji Naganawa (Department of Radiology, Nagoya University Graduate School of Medicine). The authors of this manuscript declare no relationships with any companies whose products or services may be related to the subject matter of the article. The authors state that this work has not received any funding. No complex statistical methods were necessary for this paper. Institutional review board approval was obtained. Written informed consent was waived by the institutional review board. Some study subjects or cohorts have been previously reported in 2012; Kawai Y, Suzuki K, Itoh S, et al. Autoimmune pancreatitis: assessment of the enhanced duct sign on multiphase contrast-enhanced computed tomography. Eur J Radiol 81:3055–3060. Specifically, ten focal-type autoimmune pancreatitis patients overlapped with the published study. In the previous study, only an enhancement of the main pancreatic duct wall of each patient was minutely evaluated, whereas in this study, other CT findings were additionally evaluated and regarding an enhancement of the main pancreatic duct wall, only whether present or absent was evaluated. Methodology: retrospective, diagnostic study, performed at one institution.

## References

1. Kamisawa T, Okamoto A (2006) Autoimmune pancreatitis: proposal of IgG4-related sclerosing disease. J Gastroenterol 41:613–625

2. Sahani DV, Kalva SP, Farrell J et al (2004) Autoimmune pancreatitis: imaging features. Radiology 233:345–352
3. Kawamoto S, Siegelman SS, Hruban RH, Fishman EK (2008) Lymphoplasmacytic sclerosing pancreatitis (autoimmune pancreatitis): evaluation with multidetector CT. Radiographics 28:157–170
4. Yang DH, Kim KW, Kim TK et al (2006) Autoimmune pancreatitis: radiologic findings in 20 patients. Abdom Imaging 31:94–102
5. Weber SM, Cubukcu-Dimopulo O, Palesty JA et al (2003) Lymphoplasmacytic sclerosing pancreatitis: inflammatory mimic of pancreatic carcinoma. J Gastrointest Surg 7:129–137
6. Abraham SC, Wilentz RE, Yeo CJ et al (2003) Pancreaticoduodenectomy (Whipple resections) in patients without malignancy: are they all 'chronic pancreatitis'? Am J Surg Pathol 27:110–120
7. Kamisawa T, Shimosegawa T, Okazaki K et al (2009) Standard steroid treatment for autoimmune pancreatitis. Gut 58:1504–1507
8. Shimosegawa T, Chari ST, Frulloni L et al (2011) International consensus diagnostic criteria for autoimmune pancreatitis: guidelines of the International Association of Pancreatology. Pancreas 40:352–358
9. Okazaki K, Shimosegawa T, Itoh T et al (2012) Clinical diagnostic criteria for autoimmune pancreatitis 2011 (proposal). J Jpn Pancreas (Suizou) 27:17–25
10. Ghazale A, Chari ST, Smyrk TC et al (2007) Value of serum IgG4 in the diagnosis of autoimmune pancreatitis and in distinguishing it from pancreatic cancer. Am J Gastroenterol 102:1646–1653
11. Kamisawa T, Kim MH, Liao WC et al (2011) Clinical characteristics of 327 Asian patients with autoimmune pancreatitis based on Asian diagnostic criteria. Pancreas 40:200–205
12. Levy MJ, Wiersema MJ, Chari ST (2006) Chronic pancreatitis: focal pancreatitis or cancer? Is there a role for FNA/biopsy? Autoimmune pancreatitis. Endoscopy 38(Suppl 1):S30–35
13. Bang SJ, Kim MH, Kim Do H et al (2008) Is pancreatic core biopsy sufficient to diagnose autoimmune chronic pancreatitis? Pancreas 36:84–89
14. Takahashi N, Fletcher JG, Fidler JL, Hough DM, Kawashima A, Chari ST (2008) Dual-phase CT of autoimmune pancreatitis: a multireader study. AJR Am J Roentgenol 190:280–286
15. Takahashi N, Fletcher JG, Hough DM et al (2009) Autoimmune pancreatitis: differentiation from pancreatic carcinoma and normal pancreas on the basis of enhancement characteristics at dual-phase CT. AJR Am J Roentgenol 193:479–484
16. Chang WI, Kim BJ, Lee JK et al (2009) The clinical and radiological characteristics of focal mass-forming autoimmune pancreatitis: comparison with chronic pancreatitis and pancreatic cancer. Pancreas 38:401–408
17. Sun GF, Zuo CJ, Shao CW, Wang JH, Zhang J (2013) Focal autoimmune pancreatitis: radiological characteristics help to distinguish from pancreatic cancer. World J Gastroenterol 19:3634–3641
18. Irie H, Honda H, Baba S et al (1998) Autoimmune pancreatitis: CT and MR characteristics. AJR Am J Roentgenol 170:1323–1327
19. Suzuki K, Itoh S, Nagasaka T, Ogawa H, Ota T, Naganawa S (2010) CT findings in autoimmune pancreatitis: assessment using multiphase contrast-enhanced multisection CT. Clin Radiol 65:735–743
20. Kawai Y, Suzuki K, Itoh S, Takada A, Mori Y, Naganawa S (2012) Autoimmune pancreatitis: assessment of the enhanced duct sign on multiphase contrast-enhanced computed tomography. Eur J Radiol 81:3055–3060
21. Muhi A, Ichikawa T, Motosugi U et al (2012) Mass-forming autoimmune pancreatitis and pancreatic carcinoma: differential diagnosis on the basis of computed tomography and magnetic resonance cholangiopancreatography, and diffusion-weighted imaging findings. J Magn Reson Imaging 35:827–836
22. Sugiyama Y, Fujinaga Y, Kadoya M et al (2012) Characteristic magnetic resonance features of focal autoimmune pancreatitis useful for differentiation from pancreatic cancer. Jpn J Radiol 30:296–309
23. Fujinaga Y, Kadoya M, Hamano H et al (2011) Radiologic findings of IgG4-related disease. Curr Immunol Rev 7:186–203
24. Hattori Y, Gabata T, Zen Y, Mochizuki K, Kitagawa H, Matsui O (2010) Poorly enhanced areas of pancreatic adenocarcinomas on late-phase dynamic computed tomography: comparison with pathological findings. Pancreas 39:1263–1270
25. Morana G, Cancian L, Pozzi Mucelli R, Cugini C (2010) Staging cancer of the pancreas. Cancer Imaging 10:S137–141
26. Ichikawa T, Sou H, Araki T et al (2001) Duct-penetrating sign at MRCP: usefulness for differentiating inflammatory pancreatic mass from pancreatic carcinomas. Radiology 221:107–116
27. Zamboni G, Luttges J, Capelli P et al (2004) Histopathological features of diagnostic and clinical relevance in autoimmune pancreatitis: a study on 53 resection specimens and 9 biopsy specimens. Virchows Arch 445:552–563
28. Chari ST, Smyrk TC, Levy MJ et al (2006) Diagnosis of autoimmune pancreatitis: the Mayo Clinic experience. Clin Gastroenterol Hepatol 4:1010–1016
29. Matsumoto S, Mori H, Kiyonaga M et al (2012) "Peripancreatic strands appearance" in pancreatic body and tail carcinoma: evaluation by multi-detector CT with pathological correlation. Abdom Imaging 37:602–608
30. Glaser J, Hogemann B, Krummenerl T et al (1987) Sonographic imaging of the pancreatic duct. New diagnostic possibilities using secretin stimulation. Dig Dis Sci 32:1075–1081
31. Takayama M, Hamano H, Ochi Y et al (2004) Recurrent attacks of autoimmune pancreatitis result in pancreatic stone formation. Am J Gastroenterol 99:932–937